AIRBORNE AND SPACEBORNE SAR INTEGRATION WITH TM-LANDSAT AND GAMMA RA SPECTROMETRY FOR GEOLOGICAL MAPPING IN A TROPICAL RAIN FOREST ENVIRONME

W.R. Paradella +, R.W. Pietsch ++, T. Toutin +++, P. A. Bignelli +, P. Veneziani +, V. H. Singhroy +++

+ National Institute for Space Research (INPE)
São José dos Campos, São Paulo, 12227-010 - Brazil

++ Dendron Resources Surveys Inc.
Ottawa, Ontario, K1Z 5L9 - Canada

+++ Canada Centre for Remote Sensing (CCRS)
Ottawa, Ontario, K1A 0Y7 - Canada

ABSTRACT

This paper focuses on the analysis of SAR data (C-HH airborne, JERS-1, ERS-1) digitally integrated with optical (TM-Landsat) and airborne gamma ray data for geological mapping in the Carajás Mineral Province (Brazilian Amazon Region). A methodological approach of data integration was designed, implemented and evaluated aiming at geological mapping.The Province is related to an Archean Shear Belt, with metasediments, metavolcanics, gneissesand granulites. Anorogenic granites with Middle Proterozoic ages are scattered throughout thestudy area. Radar with TM-Landsat produces an enhanced image in which spectral variations are closely related to geobotanical -relief units. TM-Landsat also enhances topographic features almost parallel to the radar illumination. Radar integrated with gamma ray also provides complementary information to the Radar/TM-Landsat images. The individual gamma channel/radar products show the relationships between terrain morphology and bedrock properties, such as rock units (Radar/Total Count) and metasomatic process (Radar/Uranium, Radar/Thorium). In multisource data integration, radiometric and geometric aspects can not be considered independently. The choice of common pixel size should be determined as a compromise between accuracy of the distinct ortho-images, and by the information content to be extracted. The spaceborne SAR data have shown, as expected, layover and foreshortening, but the effects were less severe in the JERS-1 than in the ERS-1 data. However, the ERS-1distinct azimuth angle provides some additional information regarding structures which are not so evident in the other SAR data. Results of this research emphasize the importance of using SAR integrated products for geological mapping in this environment, particularly when airborne geophysical data are available.

1.0 INTRODUCTION

It is assumed that more than 50% of the Brazilian Amazon region have already been cov aerogeophysical surveys (magnetic and gamma ray spectrometry). These efforts have broadly confirme *

---

* Presented at the Eleventh Thematic Conference and Workshops on Applied Geologic Remote Sensi Vegas, Nevada, 27-29 February 1996.

l potential of the region, particularly in the Serra dos Carajás area. The Carajás Mineral Province passes the world's largest iron deposits and the important Brazilian deposits of Salobo (Cu-Au-Mo-Ag), (Cu-Zn), Azul (Mn), Bahia (Au-Cu) and Vermelho (Ni), among others. Despite of the great volume of vailable, the geology of the Province is incompletely mapped. Areas around the main deposits have already napped in detail, but a regional integration is still necessary.

The usage of optical RS data for geological mapping has presented major drawbacks, including an almost ial cloud cover that restricts the data acquisition and the high sun-angle in the tropics, which provides only l shadowing. The thick vegetation hinders the direct interaction of solar radiation with soil and outcrops and ptical sensors cannot interact with rocks and structures directly, although geobotanical approaches can be l in some situations to infer major bedrock types (Paradella et al. 1994a). Thus, radar has played an tant role in the acquisition of geological information in this kind of terrain (Silva et al. 1974, among others). preparation for the RADARSAT and ERS-2 launches, an airborne SAR campaign (SAREX'92) was aken during April 92 in the Carajás Province. The results of these investigations have already been hed, focusing mainly on the visual analysis of the SAR data (Paradella et al. 1994b).

The digital integration of radar with optical and geoscience data (geophysical, geochemical, geological, s becoming more commonplace in the literature since multi-channel georeferenced image-maps useful for gic interpretation are feasible (Kowalik and Glenn 1987, Harris 1991, Mussakowski et al. 1991, Harris et al. Rencz et al. 1994, among others). The integration of SAR with optical data, such as TM-Landsat, offers an product in which, spectral patterns are mainly related to vegetation responses displayed as hue variations, the radar provides the enhanced topography. On the other hand, the integration of radar with raster-based ysical data provides a powerful way to visually correlate topographic variations with bedrock and structural rties.The ultimate application of these merging techniques will result in more detailed and accurate gical interpretation. Recent studies have already been carried out in the Carajás Region based on TM- at and airborne gamma ray data (Dias 1994, Martini 1995) and confirm the great potential of integrated cts as an effective tool for geological application in the region. However, the integration of airborne and borne digital SAR with optical and aerogeophysical data have not been evaluated yet. Thus, this paper ses the results obtained from the integration of SAR with TM-Landsat and gamma ray data in the Carajás al Province.

2.0. LOCATION AND GEOLOGY OF THE AREA

An area of 55 by 55 km, in the center of the Carajás Mountain Range, easternmost border of the lian Amazon Region (Pará State), was selected for the investigation (Figure 1). The area is part of a tainous and highly dissected terrain called "Serra dos Carajás" with altitudes around 700 meters and unded by northern and southern lowlands with altitudes around 150 up to 250 meters above sea level. The a dos Carajás" is part of the Amazonian Craton. The tectonical and geological evolution of the area are still ntroversy basically because the complexity of the environment and the lack of field information. Cordani and Neves (1982) proposed a tectonic model characterized by marginal mobile Proterozoic Belts surrounding an cratonic nucleus based on geochronological ages. Thus, granulitic and migmatitic rocks in the northern r of the Carajás Mountain Range would be related to the "Maroni-Itacaiúnas Belt" with Early Proterozoic and, gneisses metavolcanic and metasedimentary rocks from the "bulk"of the Carajás area would be related to Central Amazonia Province" with Early Proterozoic/Archean ages. Hasui et al. (1984) and Hasui and Haraly 5) presented an alternative model based on geophysical and structural data. In this model, the tectonical ework of the Amazonian Craton is conceived based on several independent Archean crustal blocks. The rs of these blocks are defined by positive gravimetric anomalies, strong variations in magnetic responses and ral linear trends of tectonical structures. In the nucleus of these blocks are common granitoids and volcanic- nentary sequences (type "greenstone belts"). Thus, taking into account this model, the study area would be ted in the Archean Itacaiúnas Belt, a wide WNW-ESE shear zone with metasediments, metavolcanics, ses and granulites. Araújo et al. (1988), CPRM (1991) and Costa et al. (1994) have detailed this model. The a dos Carajás" would be part of the Itacaiúnas oblique ductile shear belt composed of two main litho-

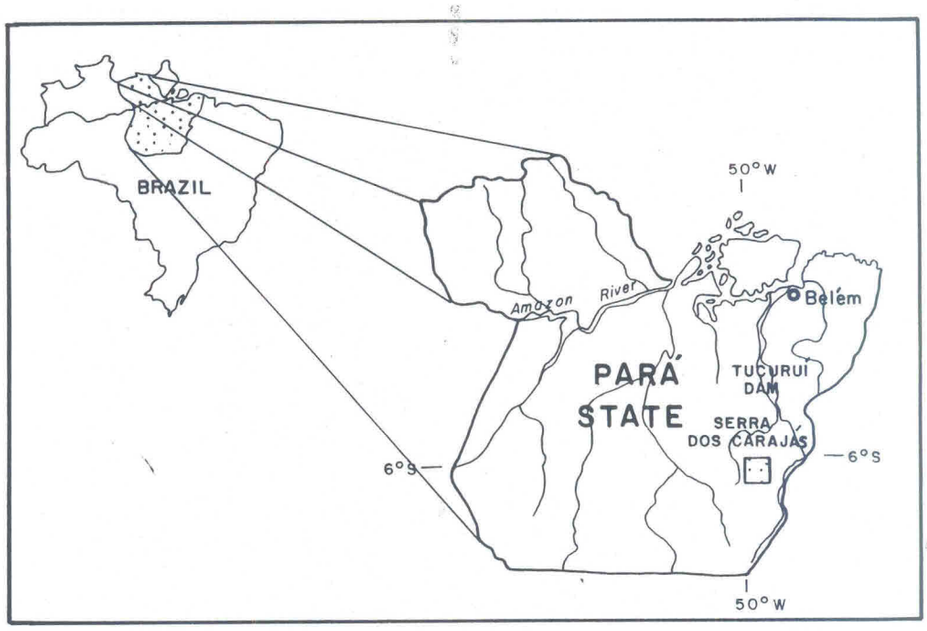

Figure 1. Location of the study area

structural domains in the area. The southern domain is typified by imbricated sinistral shear zones character by small belts and lenses of the Xingu (gneisses) and Pium (granulites) Complex, sheeted Plaquê granitoids Sapucaia (mafic and ultramafic volcanites) Group. The imbrication is related to a northeastward thrust compo plunging to the south (NNE-SSW stretched mineral lineations dipping to SSW). Due to this strong imbric process, mineralogical changes in amphibolites facies have occurred. The northern domain includes rocks Grão Pará Group (Parauapebas Formation: metabasalts and metarhyolites; Carajás Formation: banded sequences; Águas Claras Formation: metasediments) and is related to a WNW-ESE sinistral transcu (strike-slip) system represented as a "positive flower" due to a EW sinistral binary, with maximum compressi the NE-SW direction. Stretching lineations associated with thrust faults strike NE-SW, with NNE-SSW an variations, and dip to NE in the southern flank and to SW in the northern flank of the proposed "flower". T authors also proposed that the relationship between the two domains has indicated progressive oblique deform leading to the transportation of rock mass from NE to SW. This tectonic regime has resulted first in a direct (transtensional) basin, filled with volcanic, chemical and clastic sediment, followed by block rotation, transpr and formation of the regional structure now revealed by the Grão Pará Group. Anorogenic granitic intrusion across all the above cited sequences and are represented, in the study area, by the Serra dos Carajás batholith ages around 1.88 Ga). Finally, a prominent structural feature in the area is the NW-SE Carajás Fault, associa a sinistral movement and related to the latest event in the regional (directional) kinematic in the area. Part geological map from CPRM (1991), which covers the study area, is presented in Figure 2.

3.0. DATASET

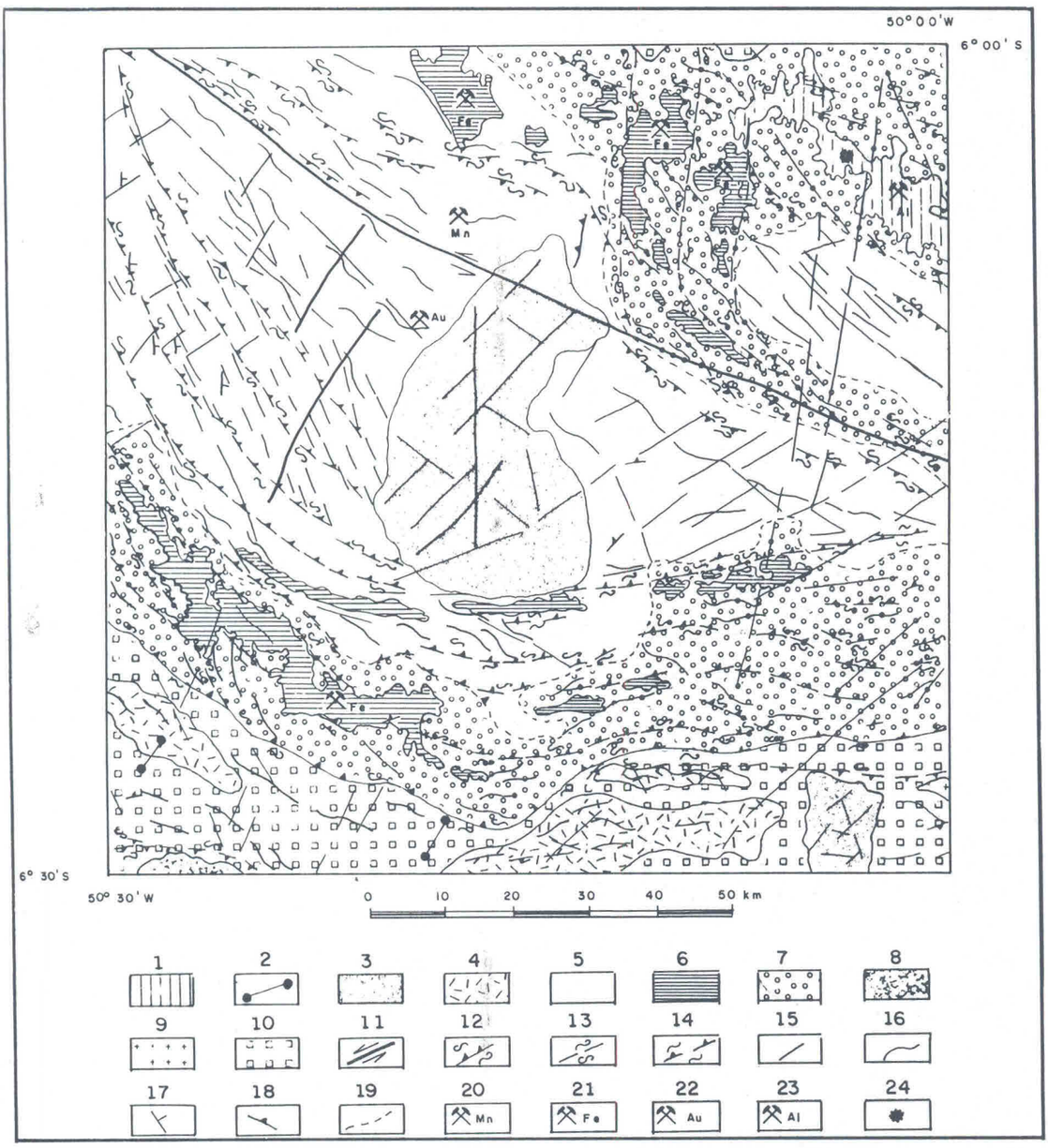

Figure 2. Geological map of the area: laterites = 1, dikes = 2, granites = 3, granitoids = 4, Águas Claras Formation = 5, Carajás Formation = 6, Parauapebas Formation = 7, Sapucaia Group = 8, Pium Complex = 9, Xingu Complex = 10, transcurrent faults = 11, shear zone with sinistral oblique thrust = 12, shear zone with indicated transcurrent movements = 13, shear zone with thrust = 14, faults/fracture = 15, geologic boundary = 16, bedding = 17, mylonitic foliation = 18, inferred geologic boundary = 19, Mn mine = 20, Fe mine = 21, Au deposit = 22, Al deposit = 23, Carajás village = 24 (Souce = CPRM 1991).

The airborne C-SAR data was acquired on April 15, 1992, and is part of one of the SAREX'92 CCRS flights (Wide Mode) over the Carajás area (C-HH, incidence angles 45 to 85 degrees). The flight was parallel to descending proposed RADARSAT track (N13E direction, looking angle N77W). The data was 8-bit detected and processed to a 7 look radiometric resolution. The spatial range and azimuth resolution were 20 and 10 m, respectively. The range sampling (pixel spacing) and azimuth sampling (line spacing) was 15 and 6.9 m, respectively. JERS-1 data was provided by ERSDAC, band L-HH, 35 degrees of incidence angle in the center of the scene. The data was acquired on March 07, 1994, descending orbit, also parallel to the airborne SAR flight. The image was 16-bit, processed to a 4 look resolution and with 30 meter spatial resolution and 12.5 by 12.5 of pixel spacing. ERS-1 data was provided by INPE, C-VV, with 23 degrees of incidence angle (center of the scene). The image was collected on June 15, 1992, on an ascending orbit (N12W, looking angle N78E). The image was georeferenced at INPE and produced at a 3 look radiometric resolution, 16-bit, spatial resolution of 30m and 12.5 by 12.5 of pixel spacing. TM-Landsat data (six reflective bands) was processed by INPE and delivered also UTM georeferenced (Path 224/Row 64). The data was acquired on June 22, 1992, with 49 and 43 degrees of sun azimuth and elevation, respectively. The spatial resolution and pixel spacing are the same (30 meters). Gamma airborne data (eU, eTh and Total Count) were provided by CPRM and were acquired in the period of 1975-1976. The K channel was not originally available. The flights were 150meter height above the terrain, north-south direction and 1 km apart. The sampling interval along the profiles was equivalent to a 65 meter distance on the surface. Three corrections were previously applied: atmospheric background, Compton, and altitude effects. The gamma units are eU (ppm), eTh (ppm) and Total Count (cps). In order to enhance the definition of the U and Th responses, these channels were also originally multiplied by a factor of 10. A previous anti-aliasing filter was also applied (frequency of 0.0004 cycles/meter). The original values were transformed to a final UTM grid file (125 meter resolution, 16 bit format) by CPRM based on the BIGRID software (linear interpolations in the NS direction and spline cubic function in the EW direction). Finally, it was also used a DEM with a 100 meter grid resolution.

4.0. METHODOLOGICAL APPROACH

The main steps in the methodological approach are represented in the flow chart of Figure 3. The pre-processing phase was carried out in two steps and corresponded to the radiometric and geometric corrections. Radiometric corrections have included Antenna Pattern (APC) for airborne data and Speckle Suppression Filtering (for all SAR data). APC was based on the procedures developed by Pietsch (1994). Fgamma filter (Lopes et al. 1990) was applied to reduce speckle effects (3 by 3 pixel window). The area has significant topographic relief and the geometric correction should take this fact into consideration. The geometric correction was based on a geometric modeling which considers the different distortions relative to the global geometry of viewing: (1) distortions relative to the platform (position, velocity, orientation); (2) distortions relative to the sensor (orientation angles, instantaneous field of view, line integration time); (3) distortions relative to the Earth (geoid-ellipsoid including elevation) and (4) distortions relative to the cartographic projection (ellipsoid-cartographic plane). The SRIT software has been developed at CCRS and details of this ortho-rectification can be found in Toutin et al. (1992).

Several enhancement techniques have been presented in the literature, aiming at the integration of remotely sensed, geophysical and thematic data for geological applications. Normally, a wide color range is desirable, and can be related to an holistic understanding of the complex association between the variables involved (vegetation, lithology, structures, geophysical properties, etc.). Harris et al. (1994) properly discussed this issue and concluded that color display based on IHS transform has presented the best overall performance when compared with other techniques. The digital integration was mainly based on the IHS transformation combined with some enhancement techniques. For the SAR/TM-Landsat integrated products, a set of TM-Bands (TM3, 4 and 5) was chosen based on the results obtained by Paradella et al. (1994a) from a feature selection routine (Optimum Index Factor) applied in the Carajás area. Decorrelation Stretch was applied to the three selected TM bands (TM 4, 5 and 3 in the RGB space) before input to the IHS transformion in the integration of SAR (airborne and JERS-1) with TM-Landsat. Linear stretched SAR channel is best used as a source of intensity information in the IHS to RGB transformation and provides the best enhanced relief. Saturation image was substituted by

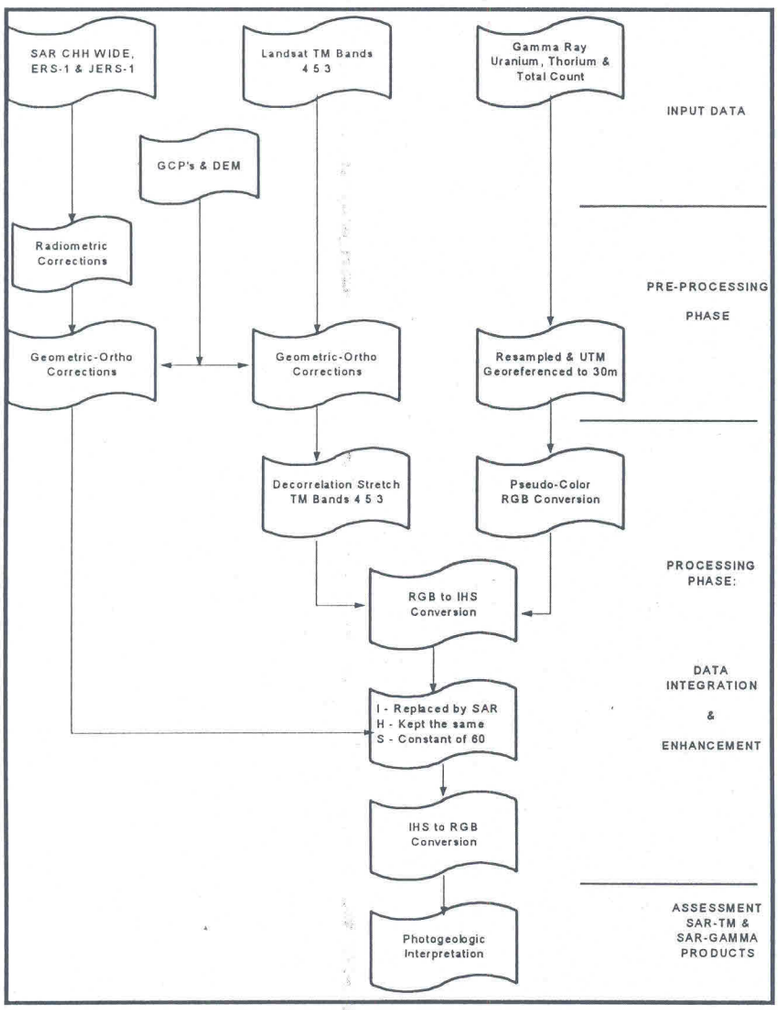

Figure 3. Flow chart with the main steps in the data integration

constant value (digital number = 60).

Multiple gamma channels (U, Th, K) are normally used to modulate hue while radar (or TM PC1) is related to intensity. In spite of the good results obtained for the Carajás area by Dias (1994) and Martini (1995), with the inclusion of the Total Count channel as a substitute for the K channel, a "bias" in the mixture of colors could not be avoided since Total Count represents the integrated surface radioactivity and a redundancy in the Th and U would be present in the final color patterns. Thus, gamma ray channels were linearly 8-bit compressed, resampled to common pixel size (cubic convolution interpolation) UTM geo-referenced and individually integrated with SAR (airborne, ERS-1 and JERS-1) through the generation of pseudo-color tables to highlight the total ranges of radiometric values. The RGB pseudo-colors channels were used as input bands in the RGB-IHS transformation. Linear stretched SAR channels were substituted in the intensity channels , hue kept the same and saturation images were substituted by a constant value.

5.0. RESULTS AND DISCUSSIONS

Although eight accurate GCPs are enough to compute the geometric modeling using SRIT softwar around 25 GCPs for each image set were used because their co-ordinates have a planimetric accuracy of 50m , an an altimetric accuracy of 25 m. Table 1 gives the root mean square, maximum and minimum errors on the GCP According to recent studies with the same geometric modeling, the RMS errors are a good indication the quality of the geometric correction, and the accuracy of the ortho-image should be around 30m for the TM Landsat and 50m for the CCRS SAR images (Toutin 1995). This discussion plays a fundamental role in the da integration, particularly in the choice of the common pixel spacing when dealing with multisource dataset. Th data integration should ensure that attributes, which are spatially and spectrally separable in the input images, a also in the output composite images. This issue has not been properly addressed in the literature. Generally, it recommended to resample each image to the lowest pixel spacing, with commensurate resolution in order to ke the spatial integrity of the higher resolution data (Harris et al. 1994). However, this is only true when the differe data have been coregistered with a sub-pixel accuracy. Previous studies have shown that a sub-pixel accuracy c generate mixed pixel in the composite image, thus creating artifacts (Toutin 1995). Keeping the spatial integrity the higher resolution data can degrade the spectral integrity of the composite image. Thus, in multisource d integration, geometric and radiometric aspects can not be considered independently. Therefore, the choice of t common pixel size was determined as a compromise between accuracy of the different ortho-images to avoid mix pixels in the composite images, and by the information content to be extracted. In order to keep a relative accura of one pixel, a 30 m pixel size has been chosen for this geological application.

Table 1. Root Mean Square, Minimum and Maximum Errors on the GCP

Platform Images	Number of GCPs	RMS Errors(m)		Minimum (m)		Maximum (m)	
		X	Y	X	Y	X	Y
TM	29	42.0	45.6	-66.8	-68.4	71.3	86.3
ERS-1	23	48.3	55.8	-73.2	-115.9	95.2	87.9
JERS-1	35	55.8	42.3	-141.7	-78.8	101.8	79.3
Wide SAR	26	74.8	26.4	-173.8	-13.8	100.5	58.0

In the Carajás Province, vegetation is the primary factor which controls the spectral responses depicte hue variations in the airborne SAR/TM-Landsat Product (Figure 4). Spectral TM responses have been relate geobotanical associations closely linked to topographic differences (elevation and slope) caused by distinct r units. The variation in the topography is largely a function rock resistance to the tropical weathering. The high most resistant ridges and plateaus, usually occur related to the banded-iron formations (Carajás Formation) metasandstones of the Águas Claras Formation, respectively. The metavolcanic component of the Pará Gr (Parauapebas Formation) is mainly associated to hilly to moderate relief while granites and migmatites/gnei (Xingu Complex) are related to low relief. The main contribution of the TM-Landsat in the integrated pro was to provide spectral variations (hues) closely related to geobotanical controls (density and stratifica variations in the vegetation related to the surface topographic expression of the geology and geomorpholo Thus, banded-iron formation areas (Carajás Formation) related to "campus rupestres",a specific savanna-vegetation, are depicted as greenish-cyan to green patterns, topographically expressed as ridges (with small la in the southwestern and northern sectors of the area. Metasediments from the Águas Claras Formation covere Tertiary laterites are related to plateaus covered by High Dense Ombrophilous Equatorial Forest and represented by pinkish-brown colors. Finally, greenshish-yellow areas, with irregular hills to low flat topogra relief, are related to the Central Serra dos Carajás granite and Parauapebas Formation metavolcanics (lo moderate biomass), respectively. Dark-blue and dark-green tones are mainly related to anthropogenic disturba in the vegetation cover (mining activities and deforestation). In addition, the TM data have also contributed in

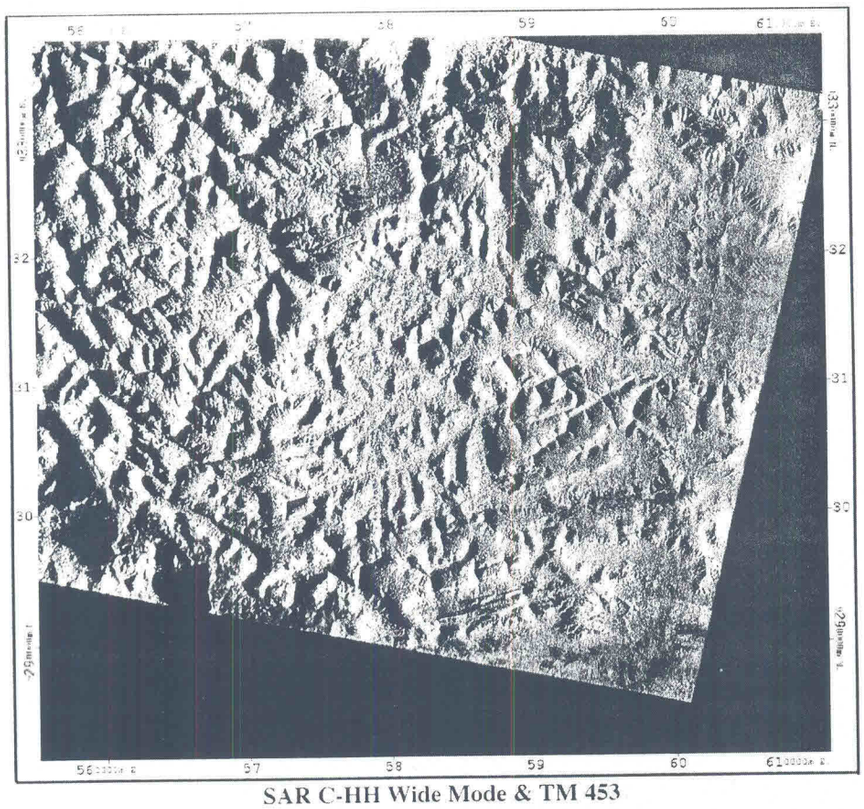

Figure 4. Airborne SAR/TM-Landsat (Bands 3,4,5) Integrated Product

enhancement of structures in the east sector (mainly structural contacts among the formations of the Grão Pará Group) and in the detection of main structures (NW-SE mylonitic foliations). This was caused by more favorable sun azimuth angle in the TM-Landsat acquisition, which is almost orthogonal, while airborne SAR data is almost parallel to the dominant NW-SE structural trend in the near range of the SAR scene. The detection of these hue variations integrated with landform expressions (relief and drainage elements defining shape, texture) and taking into consideration, (1) negative and positive linear features (indicative of bedding, foliations and fractures), (2) negative and positive ruptures (indicative of erosive and lithological limits), (3) negative and positive lineaments (indicative of major structures), and (4) boundaries of photogeological zones indicative of rock unit domains, have allowed the mapping of geological units, structures and also deformation zones in the study area.

The main contributions relating this SAR/TM-Landsat product to the previous map (Figure 3) are: (1) it was possible to map a Tertiary lateritic cover unit on the top of the plateaus (Águas Claras Formation); (2) the presence of the Águas Claras Formation rocks towards the northeastern part of the study area is not so continuos as previously mapped; (3) the characterization of distinct relief patterns as partial semi-elliptical structures in the interior of the granitic batholith suggests the presence of distinct pulses or magmatic phases in the intrusion mechanism; (4) two distinct sets of thin, continuos straight and also curvilinear features were also detected in the Águas Claras Formation area (mainly in the western sector). They were interpreted as mylonitic foliations (NW major northwest trending) and bedding (north-northwest minor trending) as previously mapped by CPRM (1991). The probability of these trends being partial expressions of basic dikes (swarm) is low based on aeromagnetic

responses; (5) small folding structures (sub-vertical axis) were also detected in the southern border of the area and they would be part of the regional kynematic model; (6) major structural lineaments were identified and were also correlated to important geological structures mapped by CPRM (1991) as oblique thrust sinistral faults (southwestern to southern trending in the SW part of the area) from the transcurrent domain of the Carajás System; (7) a prominent northwest-trending lineament was also detected and cross diagonally the area. It was interpreted as part of the major sinistral Carajás Fault system. The continuity of the topographic expression of this system through the granitic batholith strongly suggests that the Carajás Fault was reactivated after the intrusion (probably with an extensional component of movement); (8) it was also detected a photogeological unit for the Azul area. It probably represents the expression of the Igarapé Boa Sorte Formation (a sub-unit in the Grão Pará Group) as proposed by Macambira et al. (1990); (9) lineaments were also detected in the northern border (iron formations) and were correlated to NS dextral transcurrent shear zones as discussed by Marques (1991).

The IHS transformed image combining the Total Count channel and airborne SAR is presented in Figure 5. In this image , radar enhances the topography while radiometric data provides anomalies and background (radiometric landscape). In this color composition, the dark-bluish and cyan-bluish tones (low radiometric values) are related to the Parauapebas Formation (banded-iron formations and metavolcanics). The intermediate values are represented by greenish tones and are well correlated to the metasediments of the Águas Claras Formation. Finally, higher values are depicted as yellowish-red to reddish-magenta hues and are closely related to migmatites/gneisses of the Xingu Complex and anorogenic granites. Thus, the two distinct sources of data, when combined in one image product, facilitate the visual interpretation in the mapping of the main lithological units and structural patterns. Despite the fact that both are complementary products, the usage of this product decreases the "bias" and also the interpreter' s skill influence, when compared to the photogeological interpretation based on the TM/SAR product. As a consequence, the final interpretation will tend to be more reliable. The main contributions of SAR/Total Count product are: (1) it was possible to confirm the TM/SAR interpretation for the northeastern part of the area. The presence of the Águas Claras Formation rocks in this sector is unlikely to occur. The low and flat topography coupled with lower radiometric responses (dark-blue to bluish-cyan tones) than the background reflect distinct geological terrain, probably Parauapebas Formation rocks; (2) intense east-west curved topographic break associated with bluish hues (southern border of the area) can be clearly seen. This sinuous topographic belt (mainly iron- formation) marks the limit of the imbricated shear domain (to the south) with the transcurrent shear zones (to the north) of the Itacaiúnas Shear Belt. This boundary was interpreted as a thrust sinistral shear zone (Araújo et al. 1988); (3) the lithological contact between the Águas Claras metasediments and the Serra dos Carajás granite can easily be delineated. In the western border of the batholith, the regional NW foliations of the Águas Claras Formation seem to be locally affected by the intrusion and the metasediment structures inflect to NNW; (4) distinct radioelement concentrations (variations of yellow, magenta and red) closely related to distinct topographic expressions (landforms and structures) strongly favor the presence of secondary intrusives or differentiation magmatic phases within the batholith. For the northern border, the semi-elliptical structures were interpreted as limits of distinct magmatic facies. For this part of the pluton, this model is supported by recent field information (Dall'Agnoll et al. 1994) in which biotite-monzogranites and sienogranites are dominant towards the center of the batholith whereas boiotite-hornblenda-monzogranites are concentrated in the external border. The highest radiometric values in the center of the batholith are due to more K-feldspar rocks and also hydrothermal and metasomatism (intense pegmatitic manifestation). The hue and terrain variations towards the south also suggest another intrusion or magmatic differentiation (pulses); (5) the highest radiometric levels in the lower left corner of the image were also interpreted as an anorogenic intrusion and in the upper left corner to metarhyolites lavas of the Parauapebas Formation. The integration of SAR/TM and SAR/Total Count information is represented in the final map (Figure 6).

In the study area it was noticed that the Th channel is highly correlated to the Total Count channel. However, the SAR/U product has presented particular responses such as: (1) high U responses were interpreted as anorogenic granites with facies (Serra dos Carajás batholith), K-granitoid rocks, metadacites/metarhyolites affected by hydrothermal or metasomatic process. Linear zones with well defined topographic and radiometric relationships show the importance of the regional structural controls in the granitic intrusions and perhaps in the delimitation of the hydrothermal and post-magmatic activities in the study area. Additional information and future field-campaigns will be necessary to test these hypotheses. The analysis of JERS-1 and ERS-1 has shown

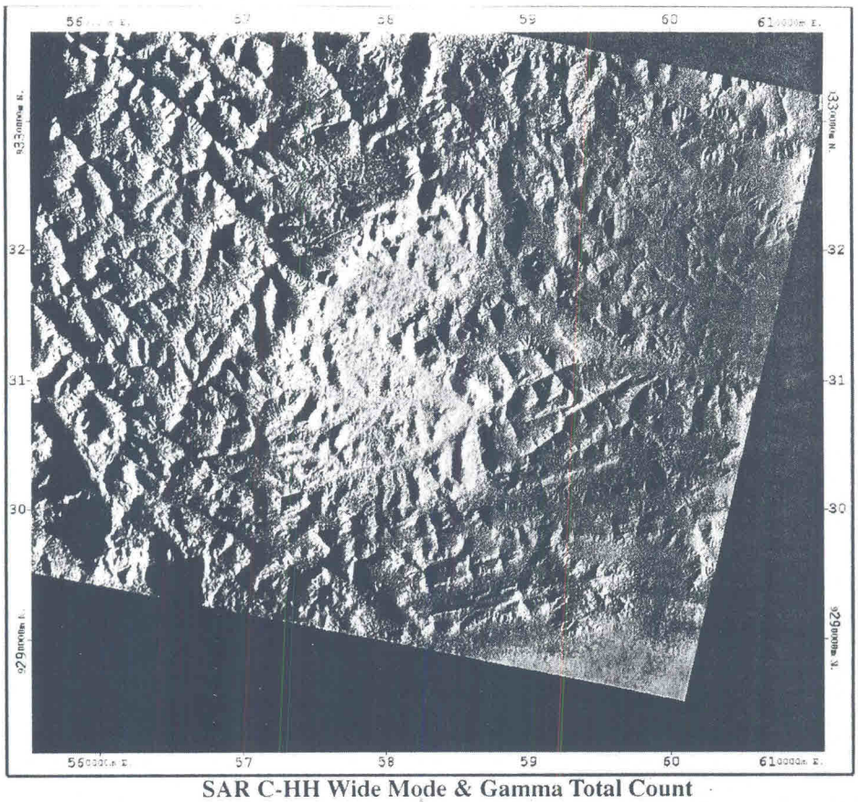

Figure 5. Airborne SAR/Total Count Channel Integrated Product

as expected, layover and foreshortening, but the effects in the JERS-1 are less severe. The integration of JERS-1 with TM and gamma provided a powerful tool for geological mapping, with highly correlated results to airborne SAR products. On the other hand, the ascending orbit of ERS-1 provide some additional information to the airborne SAR and JERS-1, particularly in the NE sector of the area (mining activities, NW-SE structures) and in the Carajás batholith (NS and NE-SW fractures).

6.0. CONCLUSIONS

A methodological approach for data integration in the tropical rainforest environment was designed, implemented and evaluated aiming at geological mapping. The combination of radar with TM-Landsat produces an enhanced product which shows spectral variations closely related to geobotanical controls displayed in gradations of hue while radar enhances the relief. As the formation of radar imagery is highly directional dependent, TM-Landsat data can also enhance topographic features almost parallel to the radar illumination. The integration of SAR with airborne gamma ray data provides another powerful tool for geological mapping with complementary information to the SAR/TM-Landsat product. It was also concluded that the integration of isolated

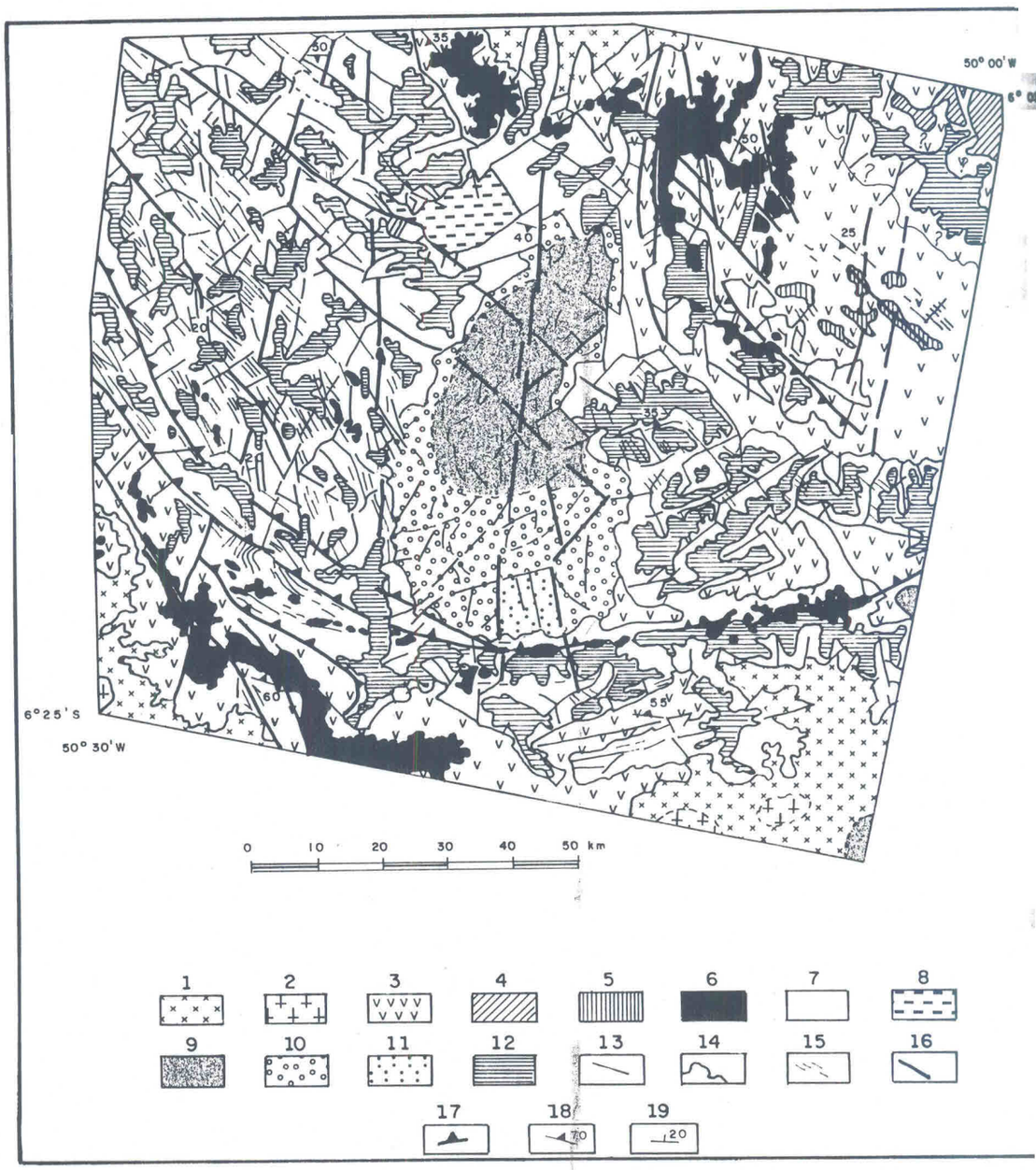

Figure 6. Final Integration Map: gneisses (Xingu Complex) = 1, granitoids (Suite Plaquê) = 2, metabasalts (Parauapebas Fm.) = 3, metarhyolites (Parauapebas Fm.) = 4, unknown (Parauapebas Fm.) = 5, banded iron formation (Parauapebas Fm.) = 6, metasediments (Águas Claras Fm.) = 7, siltites (Boa Sorte Fm.) = 8, biotite-monzo/sienogranite = 9, biotite-hornblenda monzogranite = 10, unknown (granite) = 11, laterites = 12, bedding = 13, geological boundary = 14, mylonitic foliations = 15, transcurrent faults (zone) = 16, thrust faults (zone) = 17, measured foliation = 18, measured bedding = 19 (Source: Paradella et al. 1996).

amma channel (Total Count, U, Th) is a valid alternative rather than the integration of SAR/gamma multi-annel, particularly when the original channels are partly available. The individual SAR/gamma product also vors independent insights concerning the relationships between terrain morphology/bedrock properties whether rock units (SAR/Total Count) or hydrothermal/metasomatic rock process (SAR/U, SAR/Th, etc.). In multisource ta integration, radiometric and geometric aspects should be altogether considered, particularly in the definition the common pixel size. Results of this experimental research emphasize the need of using digital integration sed on SAR data as a routine in systematic geological mapping in the Amazon Region. A large amount aerogeophysical data is available in Brazil. It can be fully explored through digital data integration in which mote sensing acts as the common link with the distinct datasets.

7.O. ACKNOWLEDGMENTS

The authors would like to acknowledge the scientific supports given by Dr. F. J. Ahern at CCRS and Dr. A. Rencz, D. Grahan and K.L. Ford at the Geological Survey of Canada (Ottawa). The investigation was also greatly benefited by the discussions with Dr. R. Dall'Agnol and J. B. S. Costa (UFPA, Belém), Dr. J. S. Bettencourt (IGUSP, S. Paulo) and the geologist O.J. B. de Araújo (CPRM, Belém). authors also thank to CPRM (R. Vasconcellos and M. L. V. de Azevedo) for providing the geophysical data. The research was funded by CNPq/Brazil (RHAE process 260050) and CIDA/CCRS (ProRadar Project). The first author would like to thank CNPq for a research grant aiming at this study. This meeting's trip funds were provided by FAPESP (Fundação de Amparo à Pesquisa do Estado de São Paulo).

8.0. REFERENCES

Araújo, O. J. B.; Maia, R. G. N.; João, X. S. J.; Costa, J. B. S. "A Megaestruturação Arqueana da Folha Serra dos Carajás". In: Geological Latin-American Congress,7, Annals, Belém, Brazil, pp: 324-338, 1988.

Cordani, U. G.; Brito Neves, B. B. "The Geologic Evolution of South America during the Archean and Early Proterozoic". Revista Brasileira de Geociências, 12 (1-3): 78-88.

Costa, J. B. S.; Araújo, O. J. B.; João, X. S.; Maia, R. G. N.; Macambira, E. M. B.; Vale, A. G.; Santos, A.; Pena Filho, J. I. C.; Neves, A. P. "Panorama Tectono-Estrutural da Região Sudeste do Estado do Pará". In: Amazon Geological Symposium, IV, Annals, Belém, pp: 314-317, 1994.

CPRM (Companhia de Pesquisa de Recursos Minerais) "Serra dos Carajás: Folha SB.22-Z-A" , Final Rept., Rio de Janeiro, Brazil, DNPM, p. 136. 1991

Dall'Agnol, R.; Barros, C. E.; Magalhães, M. S.; Villas, R. N. N.; Rios, F. J.; Nogueira, A. C.; Silva, C. M. G.; Soares, A. D. V.; Vieira, E. A. P.; Martins, L. P. B. "Estudo Petrológico da Borda Oeste do Granito Central e dos Corpos Máficos Associados à Formação Águas Claras". CVRD-UFPA, Belém, Internal Rept., p. 40, 1994.

Dias, R. R. "Avaliação de dados Aerogamaespectrométricos e de sua Integração com Imagens Digitais TM-Landsat , no Mapeamento Geológico na Serra dos Carajás (PA)", MSc Thesis in R. S., INPE, S.J. Campos, Brazil, p. 122, 1994.

Harris, J. "Mapping of Regional Structure of Eastern Nova Scotia Using Remotely Sensed Imagery: Implications for Regional Tectonics and Gold Exploration". Canadian Journal of R. S., 17 (2): 122-135, 1991.

Harris, J.; Bowie, C.; Rencz, A. N.; Graham, D. "Computer-Enhancement Technique for the Integration of remotely Sensed, Geophysical, and Thematic Data for the Geosciences". Canadian Journal of R. S., 20 (3): 210-221, 1994.

Hasui, Y.; Haraly; N. L. E.; Schobbenhaus, C. "Elementos Geofísicos e Geológicos da Região Amazônica: Subsídios para o Modelo Geotectônico". In: Geological Amazon Symposium, 1, Manaus, Annals, Vol. II, pp: 129-141, 1984.

Hasui, Y.; Haraly, N. L. E. "Integração de Informações Geofísicas e Geológicas na Definição de Estruturas Crustais Brasileiras". In: Brazilian Geological Centro-Oeste Symposium, Goiânia, Brazil, Atas.

Kowalik, W. S.; Glenn, W. E. "Image Processing of Aeromagnetic Data and Integration with Landsat Images for Improved Structural Interpretation", Geophysics, 52 (7): 875-884, 1987.

Lopes, A.; Nezry, E.; Touzi, R.; Laur, H. "Maximum a Posteriori Filtering and First Order Texture Models in SAR Images". In: IGARSS'90, Proceedings, Washington, USA, pp: 2409-2412, 1990.

Macambira, J. B.; Ramos, J. F. F.; Assis, J. F. P. ; Figueiras, A. J. M. "Projeto Pojuca". DNPM/DOCEGEO/UFPA Final Rept., Belém, Brazil, 1990.

Marçal, M. S. "Aspectos Lito-Estruturais das Minas de Ferro N4E e Manganês do Azul, Serra dos Carajás (PA)" MSc Thesis in Geology, UFPA, Belém, Brazil, p. 135, 1991.

Martini, J. M. "Análise Integrada de Dados Aplicada ao Estudo Metalogênico da Serra dos Carajás, PA". MS Thesis in Geoscience, UNICAMP, Campinas, Brazil, p. 121. 1995.

Mussakowski, R.; Trowell, N. F.; Heather, K. B. "Digital Integration of Remote Sensing and Geoscience Data fo the Goudreau-Lochalsh Area, Wawa, Ontario". Canadian Journal of Remote Sensing, 17 (2): 162-173, 1991

Paradella, W. R.; Silva, M. F. F.; Rosa, N. A.; Kushigbor, C. A. "A Geobotanical Approach to the Tropical Ra Forest Environment of the Carajás Mineral Province (Amazon Region, Brazil), Based on Digital TM-Landsat ar DEM Data" International Journal of Remote Sensing, 15 (8): 1633-1648, 1984a.

Paradella, W. R.; Liu, C. C.; Veneziani, P. Santos, A. R.; Bignelli, P. A.; Dias, R. R. "An Overview of SAREX 92 (South American Radar Experiment) Data Acquisition and Preliminary Results from Carajás Mineral Provin (Brazilian Amazon Region)". In: Tenth Them. Conf. on Geol. R. S., San Antonio, USA, Vol. II, pp: 214-22 1994b.

Pietsch, R. W. "TFI SAR Processing Procedure". Dendron Resources Surv. Inc., Inter. Rept., Canada, p. 7, 199

Rencz, A. N.; Harris, J. Watson, G. P.; Murphy, B. "Data Integration for Mineral Exploration in the Antigon Highlands, Nova Scotia: Application of GIS and RS". Canadian Journal of Remote Sensing, 20 (3): 257-267, 19

Silva, G. G.; Lima, M. I. C.; Andrade, A. R. F.; Issler, R. S.; Guimarães, G. "Folha SB-22 Tocantins: Geolog Geomorfologia, Solos, Vegetação e Uso Potencial da Terra". Projeto RADAM, Rio de Janeiro, Vol. 4, 1974.

Toutin, T.; Carbonneau, Y.; St. Laurent, L. "An Integrated Method to Rectify Airborne Radar Imagery Us DEM". Phot. Eng. and R. S., 58 (4): 417-422. 1992.

Toutin, T. "Multisource Data Integration with an Integrated and Unified Geometry Modeling". In: Sensors Environmental Applications of Remote Sensing, Askne (Ed.), Proceedings, 14th. Symposium, Rotterdam, 163-496, 1995.